Effect of different fillers on the biodegradation rate of thermoplastic starch in water and soil environments

Effect of Different Fillers on the Biodegradation Rate of Thermoplastic Starch in Water and Soil Environments

Markéta Julinová[*1], Dana Rouchalová[1], Ludmila Vaňharová[1], Pavel Skácelík[1], Martin Jurča[1], Antonín Minařík[2], Petr Duchek[3], Jana Kavečková[1]

[1]Department of Environmental Protection Engineering, Faculty of Technology, Tomas Bata University in Zlín, Vavrečkova 275, 760 01 Zlín, Czech Republic
[2]Department of Physics and Materials Engineering, Faculty of Technology, Tomas Bata University in Zlín, Vavrečkova 275, 760 01 Zlín, Czech Republic
[3]Research Centre of New Technologies, University of West Bohemia, 306 14 Plzeň, Czech Republic

Markéta Julinová julinova@utb.cz, Antonín Minařík minarik@utb.cz, Petr Duchek jduchekpe@kmm.zcu.cz

Abstract

This work investigates the effect of filler type on the rate of biodegradation of thermoplastic starch-based films in water and soil environments. The authors applied the casting method to create films of thermoplastic starch, based on waste paper, filled with clays or organic fillers. Since such materials made from cellulose tend to absorb water, we hydrophobized the surfaces of the filled thermoplastic starch samples. The structures of the blends were characterized by infrared spectroscopy, while atomic-force microscopy was applied to observe change in surface topography and the distribution of the filler. We also studied moisture resistance of the blends. Biodegradation tests revealed that surface topography, distribution of the filler and starch-to-filler interactions were non-critical to the rate and degree of biodegradation of the blends. The biodegradation rate of the blends was strongly affected by the environmental conditions (relative humidity 54%, 100%, respectively; temperature 25 °C, 37 °C, respectively). Under anaerobic conditions, it was the mixtures that biodegraded to the greatest extent, whereas the hydrophobized mixtures did so the least.

Keywords: Biodegradation, thermoplastic starch, clay, waste paper, sludge

Introduction

Over the years, attention has primarily been paid to the role of starch in the creation of biodegradable plastics from renewable resources. One reason for this is that said natural polymer is fully biodegradable in a wide range of environments. Moreover, it is popular due to being generally available and possessing low processing costs. Previously, starch was limited to application as a filler in a polymer matrix (usually at the content of 6-15%). Nonetheless, it has since become widely deployed as a packaging material, especially in thermoplastic form [**1**].

Thermoplastic starch (TPS) is a material initiated by partial disruption to the starch-grain structure. This process takes place under thermal and mechanical strain, and involves the use of suitable plasticizers. Consequently, reduced crystallinity and a lower melting point are obtained, thereby lending the

resultant starch the desired thermoplastic properties [**2**]. The composition of TPS usually comprises 50-90% starch and 10-50% plasticizers [**2, 3**].

However, some disadvantages of TPS have been identified, including retrogradation [**4**] and unsatisfactory mechanical properties under wet or dry conditions. Another issue is brittleness, caused by a high glass-transition temperature. Such brittleness can increase through autonomic release of the plasticizers initiated by the material ageing. Furthermore, it has been found that materials with a high content of amylases in their structure have a negative influence on the properties of TPS. This is induced by the linear structure declining in flexibility, hence the resultant products are more brittle than, for example, materials containing a greater amount of amylopectin [**5**]. Structural changes have also been observed during the storage of TPS and its ageing under such conditions. These are caused by the release of plasticizers and water from the structure, resulting in increased crystallinity; such changes are manifested through the material demonstrating greater rigidity [**2**]. Therefore, research has primarily been devoted to improving the properties of TPS by employing environmentally friendly inorganic or organic fillers [**3, 6**].

The most frequently utilized inorganic fillers are mineral clays [**7, 8**], which can be subdivided into several groups; for example, smectite clays (i.e. montmorillonite) or a category of materials based on kaolinite. In addition to blends discussed later in this text, other combinations that have been prepared include organic modified montmorillonite— Cloisite 6A, Cloisite 10A and Cloisite 30B [**9**], calcium bentonite [**8**], acid-modified kaolinite and acid-modified vermiculite [**10**], talc nanoparticles [**11**] and sepiolite [**12**]. Nevertheless, little attention has been paid to the influence exerted by clay type and particle distribution on the biodegradability of these materials, despite the fact that these factors affect both water solubility and uptake as well as the speed and extent of biodegradation.

In a related context, Magalhäes and Andrade [**7**], and also Bootklad and Kaewtatip [**13**], studied the biodegradability of TPS-based materials filled with clay minerals.

To date, waxes have been investigated as organic fillers for TPS, whereas less attention has been paid to chitin and chitosan [**14**]. However, the majority of research has been devoted to fillers based on cellulose in various structural forms, such as nanocrystals [**4, 15**], microcrystals, microfibres, plant cellulose and bacterial cellulose (*Acetobacter xylinum*) [**16**]. A finding shows that cellulose in the form of a microfibre or microcrystal has a significant influence on the water solubility of TPS. Bacterial cellulose exhibits extremely high strength and crystallinity as well as a very pure nanofibre structure [**16**]. Due to these properties, it is widely applied in the development of materials, while application in biomedicine has arisen as a consequence of its biocompatibility. In general, TPS supplemented with cellulose exhibits greater toughness and thermal stability, in combination with reduced solubility, in a water environment [**15, 16**].

Having consulted studies by Magalhaes and Andrade [**7**], Bootklad and Kaewtatip [**13**], Dogossy and Czigany [**17**] and Prachayawarakorn et al. [**18**], who all point out the importance of biodegradation tests in the development of TPS materials, we set out to investigate the effect that types of inorganic and organic filler exert on the biodegradation rate of thermoplastic starch-based films. The inorganic fillers utilized were commercial mineral clays, the particle sizes of which were at micro/nanoscopic scale. The literature states that this form of micro-/nano-filler enhances mechanical and user properties, hence broadens the scope of potential application of such materials. The organic fillers selected for this study were waste organic materials based on cellulose sourced from waste paper. Due to the fact that thermoplastic starch filled with materials made from cellulose tend to absorb moisture, blends were prepared and tested that had been hydrophobized by spraying the material with a hydrophobization solution (boiled linseed oil). Changes in surface topography and surface filler

distribution (the phase contrast) of the blends were characterized on an atomic force microscope (AFM). Resistance to moisture and its relation to the type of filler was also analysed. All such properties are considered important parameters for study in materials that could be used in different environments.

Experimental

Materials and Chemicals

Native potato starch was provided by Lyckeby Amylex (Czech Republic) with an amylose content of 25% and granule size of 10-100 pm. Glycerol was sourced from Lach-Ner s.r.o., Neratovice (Czech Republic). Six types of industrial minerals were utilized as the inorganic fillers (see Table **1**). The organic filler selected was post-consumer, waste newspaper material mixed with maximally 10% wt. of cuttings of laboratory filter paper, in order to simulate the real batch composed of both the recycled paper with print and without printing. All the materials were applied in their original form, i.e. without any additional processing and/or recycling, and the newspaper waste contained ink print. Boiled linseed oil (BLO) P6420 (Barvy a laky Hostivař, Czech Republic) was used for hydrophobization purposes without further treatment.

The remainder of the chemicals employed were of analytical purity, the source of these being Pliva Lachema Brno (Czech Republic).

Preparation of the Blends

The tested materials (foils) were prepared from the starch/ glycerol/filler blend in accordance with a casting method [**19**]. See Table **2** for basic description of the mixtures and their composition.

Preparing the inorganic fillers: Clay fillers (Cloisite Na, Sabenil, Lutila and kaolin) were delaminated in distilled water by adding 2 g of filler into 98 g of water under vigorous stirring for a minimum of 12 h. Due to the lamellar structure of the given clay minerals (montmorillonite and kaolinite), delamination of their mineral architecture occurred, providing single platelets of minerals at the scale of nanometers, which was advantageous in relation to the mechanical properties of the composite material. To achieve optimal delamination of the clay minerals, this water suspension was stirred for at least 24 h. The remaining two mineral fillers (silica and diatomite, respectively) were prepared in an identical manner to the clay material, but no delamination in the intrinsic structure was observed.

Table 1 Basic description of the different inorganic fillers

Designation	Clay	Description
In-water dispersible clay fillers (lamellar structure)		
MMT	Cloisite® Na^+	Natural sodium montmorillonite, d-spacing $d_{001} = 11.7$ Å, Southern Clay Products Inc., USA
S-B	Sabenil® bentonite	Soda activated bentonite, content of montmorillonite = 65–80%, also SiO_2, Al_2O_3, Fe_2O_3, d-spacing $d_{001} = 12.6$ Å, Keramost a.s. Most, Czech Republic
Lu-B	Lutila® bentonite	Non-activated bentonite in native form, content of montmorillonite = 75%, d-spacing $d_{001} = 12.5$ Å, Keramost a.s. Most, Czech Republic
Ka	Kaolin	Native form, in composition—74% kaolinite, 14% mica, 11% silica, d-spacing $d_{001} = 7.12$ Å, LB Minerals s.r.o., Horní bříza, Czech Republic
In water non-dispersible fillers		
SiPow	Silica	In powder form, particle size 0.2–0.3 µm, Czech Republic
Di	Diatomite	In composition—89.5% SiO_2, 3.9% Al_2O_3, 1% CaO, Borovany u Českých Budějovic, Czech Republic

Table 2 Composition and characteristics of TPS matrix and blends

Sample name	Starch (g)	Glycerol (g)	Filler (g)	BLO	Thickness (mm)	sCOD[a] (mg g^{-1})	TOC[b] (%)
TPS	35.0	15.0	–	–	0.120 ± 0.003	1064 ± 21	39.37 ± 0.79
TPS MMT	33.6	14.4	2	–	0.064 ± 0.004	1087 ± 22	36.91 ± 0.74
TPS Lu-B	33.6	14.4	2	–	0.099 ± 0.002	1007 ± 20	37.22 ± 0.74
TPS S-B	33.6	14.4	2	–	0.102 ± 0.002	952 ± 19	39.07 ± 0.78
TPS Ka	33.6	14.4	2	–	0.092 ± 0.001	987 ± 23	36.98 ± 0.73
TPS Di	33.6	14.4	2	–	0.111 ± 0.003	1022 ± 20	37.37 ± 0.75
TPS SiPow	33.6	14.4	2	–	0.103 ± 0.003	1058 ± 21	40.68 ± 0.81
TPS WP	32.2	13.8	4	–	0.127 ± 0.002	1118 ± 22	40.24 ± 0.80
TPS WP BLO	32.2	13.8	4	Yes	0.188 ± 0.002	920 ± 17	52.78 ± 1.06

Amounts for one batch of the casted film

[a]Solid chemical oxygen demand

[b]Contents of total organic carbon

Preparing the organic (paper) filler: 4 g of shredded waste newspapers/cuttings of filter paper were mixed thoroughly with 246 g of distilled water in a laboratory mixer (speed 1000 s^{-1}; ETA, Czech Republic).

Preparing the casting film (for the matrix only and/ or inorganic fillers): 500 mL of water was poured into a 1000 mL beaker equipped with an efficient stirrer, followed by 100 mL of the filler suspension. The mixture was stirred for 5 min (at 800 min^{-1}). Subsequently, potato starch and glycerol were added to this mixture and the volume was fixed at 700 mL by water. The suspension was heated up to 50 °C (rate 1 °C min^{-1}) with the stirrer set to a lower speed (180 min^{-1}). Upon exceeding the temperature of 50 °C (water bath, digital magnetic stirrer, TRP350-RP hot plate, Miulab, China), stirring was slowed down to 100 min^{-1} to prevent excessive breakage of the long polysaccharide chains; such breakage would have the potential to diminish the mechanical properties of the resulting material. At about 75 °C, the process of starch gelatinization commenced, evident from apparent thickening of the reaction mixture. This continued to approximately 80 °C under moderate stirring conditions. We observed that the starch grains had opened fully after 20 min, and the highly viscous material possessed amorphous

properties. The final step was to degas the TPS starch in a desiccator with the aid of a water pump the instant that maximal thermoplasticity of the starch component had been reached. Evacuation of the hot reaction mixture proceeded continuously from the atmospheric pressure down to 0.7-2 kPa within 3 min. Processing it took about 5 min under natural cooling conditions. This proved indispensable, as detrimental air bubbles were removed from the liquid phase, yet the viscosity of the composite material remained suitable for the subsequent casting process.

The same preparation procedure was followed for compositions with the organic filler, except the amount of water poured into the 1000 mL beaker equalled only 400 mL. 250 g of the organic filler suspension was added into it and then mixed with the starch and glycerol components, exactly according to the methodology employed for the mineral fillers.

Casting the material: The homogeneous matrix (TPS) and the composite were cast on a PVC pad (dimensions 297 X 420 mm) using a jig with height of the cast 3.1 mm. The casted plastic films were dried under open-air conditions at 24.1 ± 0.7 °C and a relative humidity of 23.6 ± 0.8%. Overall, the films were dry enough to separate from the pad 72 h after being cast. The cast film was reproduced in triplicates for each composition.

Hydrophobization: We used boiled linseed oil (BLO) P6420 (Barvy a laky Hostivař, Czech Republic) for the hydrophobization stage without further additional treatment. It was performed by simply dipping the prepared samples (TPS + filler) into the BLO, removing any excess oil and drying them in the open air. The amount of hydrophobic media deposited lay in the range 1.2—1.4 g dm^{-2} of the treated surface.

One sample film (test specimen) was taken from each instance of casting and applied in characterization and biodegradation tests.

Attenuated Total Reflectance Infrared Spectroscopy (FTIR-ATR)

The FTIR-ATR spectra of the TPS and blends prior to and following the biodegradation test were recorded on a Nicolet iS10 device (Thermo Scientific, USA), fitted with an ATR Smart MIRacle™ adapter containing a diamond crystal; the spectral range encompassed 4000 cm^{-1} to 525 cm^{-1}, at the resolution of 4 cm^{-1}, and the number of scans totalled 32. The spectra obtained were processed via Omnic 8 software (Thermo Scientific, USA) [**20**].

Atomic Force Microscopy (AFM)

Changes in surface topography and phase contrast were characterized on an Ntegra-Prima atomic force microscope (NT-MDT Spectrum Instruments, Moscow, Russia). Measurements were performed at the scan speed of 0.5 Hz, at the resolution of 512 X 512 pixels, in tapping mode at room temperature in an air atmosphere. Additionally, a silicone-nitride probe with a resonant frequency of (150 ± 50) kHz and stiffness constant of 5.1 N m^{-1} (NSG01, NT-MDT) was utilized. The amount of filler at the surfaces was gauged by analysing phase images with ImageJ 1.8 software (Wayne Rasband, National Institutes of Health, USA). The extent of surface roughness **Sa** (the arithmetical mean maximum, this constituting an absolute value—the difference in height of each point compared to the arithmetical mean for the entire surface of the sample) was obtained via Gwyddion 2.5 software (Czech Metrology Institute).

Scanning Electron Microscopy (SEM)

The effect of biodegradation upon the polymer surfaces was examined by scanning electron microscopy. Analysis took place on a Phenom Pro scanning electron microscope (Phenom-World BV, Eindhoven, Netherlands). The samples were observed at acceleration voltages ranging between 5 and 10 kV in backscattered electron mode; the scope of magnification comprised X 1000 to X 10000. Measurements were carried out on samples without prior metallization, employing a special sample holder for the aforementioned Phenom Pro unit.

Water Uptake Test

The water uptake was determined gravimetrically. Samples of TPS and the blends (stored at room temperature) at the given dimensions (10 mm X 10 mm) were weighed out and placed in a humidity chamber (54% RH, 25 °C; 100% RH, 25 °C). The difference in weight was measured at specified time intervals until no weight change (± 0.001 g) was observed [**21**]. Afterwards, the extent of water uptake in per cent was calculated according to the following Eq. (**1**):

$$\text{Water uptake} = \left[\left(M_f - M_i\right)/M_i\right] \times 100 \quad (1)$$

where M_f is the final mass of the sample and M_i is the initial mass of the sample (both in g).

Water Solubility

Samples of TPS and the blends were immersed in 300 mL of distilled water (at an initial concentration of 200 ± 5 mg l^{-1}); the system was continuous mixing (200 rpm) at 25 °C or 37 °C. At the designated time, 1 mL of the solution was removed by pipette and tested to determine the concentration of the solution by determining the chemical oxygen demand. From these values the dissolution characteristics of the samples were calculated according to the following Eq. (**2**):

$$\text{Water solubility} = \left(COD_{DISSOLVED}/sCOD_{SAMPLE}\right) \times 100 \quad (2)$$

where $COD_{DISSOLVED}$ is the concentration of the dissolved TPS or blend expressed as chemical oxidation demand (COD), and $sCOD_{SAMPLE}$ is the experimental determination of the solid chemical oxygen demand of the TPS or blend (both in mg g^{-1}) [**22**].

In accordance with a previous work by us [**22**], the procedure for calculating the solid COD [**23**] of the TPS or blends (sCODBLENDS) involved the following: 2-3 mg of the sample (measured on a Mettler MX-5 microbalance, Toledo International Inc., USA) were transferred to test tubes with screw caps containing 2 mL of distilled water. Afterwards, they were digested (2 h, 150 °C) according to the international standard colourimetric method—ISO 15,705:2002 [**24**]; the small-scale sealed-tube approach was adopted to work out the chemical oxygen demand index. The COD was determined through applying potassium dichromate via the closed reflux method [**23**]. Mercuric sulphate was employed to mask chloride interference, while silver sulphate was dissolved in concentrated H_2SO_4 to act as a catalyst. All of the reagents were of analytical grade [**22**].

Biodegradation in an Aqueous Aerobic Environment

The biodegradability of TPS and the blends in an aqueous aerobic environment was studied in the presence of a mixed microbial culture, supplied in the form of activated sludge from the given municipal wastewater treatment plant. Biodegradation was investigated on a MicroOxymax $O_2/CO_2/CH_4$ microrespirometer (Columbus Instruments Corp., USA).

The mineral medium was prepared by pouring 800 mL of aerated distilled water into a 1 l bottle and then adding the following stock solutions at 1 mL each: $CaCl_2$ (27.5 g l^{-1}), $FeCl_3$-$6H_2O$ (0.25 g l^{-1}) and $MgSO_4$-$7H_2O$ (22.5 g l1); as well as solutions of the trace elements: H_3BO_3 (0.75 g l^{-1}), $(NH_4)_6Mo_7O_{24}$-$4H_2O$ (0.05 g l^{-1}), $CoSO_4$-$7H_2O$ (0.18 g l^{-1}), $CuSO_4$-$_5H_2O$ (0.5 g l^{-1}), $ZnSO_4$-$7H_2O$ (0.1 g l^{-1}) and $FeSO_4$-$7H_2O$ (3 g l^{-1}). In addition, 20 mL of phosphate buffer was added (8.2 g l^{-1} KH_2PO_4, 21.75 g l^{-1} K_2HPO_4'$12H_2O$, 44.7 g L^{-1} Na_2HPO_4·$12H_2O$) along with 5 mL of $(NH_4)_2SO_4$ (10 g L^{-1}). After being mixed, it was supplemented with aerated distilled water to top it up to 1 litre.

The initial dry matter concentration of the activated sludge equalled 500 mg l^{-1}, while the substrate was 200 mg l^{-1}. The substrate—either TPS or a blend—was dosed directly into the reaction suspension. The mineral medium was utilized when preparing the activated sludge suspension. Initially, the level of pH stood at 7.0 ± 0.5. Samples of the suspension for determining the pH and dry matter of the biomass were always withdrawn at the start and end of the test. Concurrently, we investigated the aspect of endogenous respiration. When CO_2 release levelled off and remained constant (a plateau phase) and no further biodegradation was expected, the test was considered complete.

The basic biodegradability criterion was the ratio of CO_2 actually produced during microbial breakdown to the theoretical quantity of CO_2, as given by the balance of carbon present in the sample, which was expressed as D_{CO2} (%) in accordance with the Eq. (**3**):

$$D_{CO_2} = \left[\left(n_{SAMPLE} - n_{BLANK}\right)/Th\right] \times 100 \qquad (3)$$

where n_{SAMPLE} is the quantity of CO_2 produced during breakdown of the substrate [mmol], n_{BLANK} is the quantity of CO_2 produced during endogenous respiration of the microorganisms [mmol] and Th is the theoretical production of CO_2 from total substrate breakdown [mmol], as determined by the balance of organically bound carbon in the tested material; see Table **2**; we utilized a TOC SSM-5000A device for this purpose (Shimadzu Corp., Japan) [**22**].

Biodegradation in the Aqueous Anaerobic Environment

The biodegradability of TPS and the blends in the aqueous anaerobic environment was studied in the presence of a mixed microbial culture, supplied in the form of partially digested sludge, which was derived from anaerobic stabilization of residual activated sludge from the given municipal wastewater treatment plant in a method according to a previous work [**25**].

The initial concentration of the anaerobic sludge dry matter equalled 5 g l^{-1}, and that of the blends was approximately 500 mg l^{-1}. The filled bottles were bubbled through with nitrogen for approximately 5 min, sealed gas-tight with stoppers equipped with septa and immersed in a water bath tempered to 37 ± 1 °C. The contents of the bottles were continuously stirred during the experiment. The extent of anaerobic biodegradability was gauged through the quantity of CO_2 and CH_4 produced. Both gases were subjected to final analysis by gas chromatography (on an Agilent GC 7890A unit equipped with a PORAPAK Q column and TCD detector, with helium as the carrier gas at 50 mL min^{-1}, $T_{inject0r}$ = 200 °C,

T_{OTen} = 35 °C, T_{det} = 220 °C). A sample of the gaseous phase was taken, via a septum, from the sealed gas-tight bottle wherein the process of anaerobic degradation was ongoing; a gas-tight syringe was utilized for this purpose (Hamilton, USA; dispensing volume: 100 pl). 100 pl of the gaseous phase was subsequently injected into an injector (temperature: 200 °C) via a gas chromatograph septum. When a constant level of CO_2 and CH_4 release was attained (a plateau phase reached) and no further biodegradation was expected, the test was considered complete.

Anaerobic biodegradation in per cent (DCH_4) was evaluated according to the Eq. (**4**):

$$D_{CH_4} = \left[\left(w_{SAMPLE} - w_{BLANK}\right) / \left(w_{SAMPLE} \times TOC\right)\right] \times 100 \quad (4)$$

where w_{BLANK} represents production (mg) of carbon in the form of carbon dioxide and methane in the blank (endogenous production), w_{SAMPLE} represents production (mg) of carbon in the form of carbon dioxide and methane in the sample during biodegradation of the tested material, TOC (%) is the organically bound carbon in the tested material (Table **2**) and w_{SAMPLE} is the weight of the tested material (mg).

Biodegradation in Soil

The biodegradation of TPS and the blends were studied by conducting respirometric tests (on a BI-2000 electrochemical respirometer - Bioscience Inc., USA) and soil-burial tests [**20**].

Biologically active soil sourced from a forest was purged of coarse fractions by sieving; its inherent moisture was ~ 55% and the content of organic carbon in solid phase was 16.9 ± 1.36% (Shimadzu TOC 5000A—SSM, Shimadzu Corp., Japan). The microbial activity of the soil was characterized by microbiological soil analysis. Other data comprised the total number of bacteria: 5 0.106 CFU. g^{-1}; total number of gram-negative bacteria: 6.3 0.105 CFU. g^{-1}; total amount of soil mould: 14 0.103 CFU.g^{-1}; and the content of actinomycete: 5.105 CFU.g^{-1}.

Respirometric Tests

The chosen method involved determining biological oxygen demand (ISO 17,556:2012) [**26**] on the BI-2000 electrochemical respirometer (Bioscience Inc., USA). In accordance with a previous work by us [**19**], we followed the steps described below to prepare the experiments; the biodegradation tests were performed in a 1000 mL glass respirometric flask. Firstly, 250 mL of soil was dosed into the flask, 1 g of the sample in the form of a small piece (5 x 5 mm) of film was then added, which was then covered with another 250 mL of the soil; hence, the total volume of the soil in the respirometric flask equalled 500 mL. The soil tests were conducted at 25 ± 1 °C. All measurements were conducted four times in parallel. When a constant level of BOD was attained (a plateau phase) and no further biodegradation was expected, the test was considered complete.

The percentage of biodegradation was calculated according to the Eq. (5):

$$D_{BOD} = \left[\frac{\left(BOD_{SAMPLE} - BOD_{BLANK}\right) / w_{SAMPLE}}{sCOD}\right] \times 100 \quad (5)$$

where BOD_{blank} represents biological oxygen demand (mg) in the blank (endogenous respiration), BOD_{sample} represents biological oxygen demand (mg) in the sample during biodegradation of the tested material, sCOD is the chemical oxygen demand (mg g^{-1}) of the tested material (Table **2**) and w_{SAMPLE} is the weight of the tested material (g).

Soil Burial Tests [20]

In order to assess the biodeterioration of the TPS and blends in the presence of soil microorganisms, a soil reactor designed by Rizzarelli et al. [**27**] was utilized. The experiments were carried out in an aerobic environment at 25 ± 1 °C, under the controlled moisture of approximately 55%. The tested materials (2 x 2 cm; initial weight 45-70 mg) were sandwiched between two layers of a mixture of milled perlite (650 g) and of soil (8 l). Samples in the form of test pieces were placed in the soil so that the minimum thickness of the soil layer above and below the sample was 4 cm and the least horizontal distance between the samples was 1 cm. Perlite (a heat expanded aluminosilicate) was added to encourage aeration of the soil and the amount of water retained. A flow of moistened air was supplied from the bottom of each vessel every 2 h for 15 min.

During the test, the samples were removed from the soil, brushed softly and dried at room temperature until constant weight was achieved. FTIR analysis was then carried out along with visual assessment.

Mathematical Description of Experimental Data

The course of biodegradation over time for the TPS and blends, D = f(t), was described by regression, applying an equation for first-order substrate kinetics (Eq. **6**) [**28**]. We calculated regression coefficients by applying the least squares method with Statistica CZ 6.1 software.

All the experimentally obtained dependencies of D_{CO2} = f(t), D_{boD} = f(t) and DCH_4 = f(t) were regressed, so the only values subsequently taken into account were those clearly involving biological degradation (after the lag phase) [**29**]. In the resultant regression analysis, the regression coefficient > 0.96 (n = 3) was always achieved.

$$D = D_{max} \times \left[1 - e^{-k \times (t - t_{lag})}\right] \quad (6)$$

where D_{max} is the regression coefficient representing the limit value in infinite time (%), k represents the constant rates of k_{DBOD}, k_{DCH4} and k_{DCO2} (in h^{-1}) and t_{lag} is the shift on the time axis expressing the lag phase (h).

Predicting the environmental fate of the TPS and blends requires knowledge of the overall degradation half-life time of each compartment. Such a half-life time can be expressed as (Eq. **7**):

$$t_{1/2} = \ln 2 / k \quad (7)$$

where k—k_{DBOD}, k_{DCH4} and k_{DCO2} (h^{-1})—represent first-order rate constants for biodegradation, determined according to Eq. **6**.

Statistical Analysis

The data underwent one-way analysis of variance (ANOVA) with the Tukey-Kramer multiple comparisons test for 95% reliability, revealing significant differences between the samples [**30**]. These variations were considered significant when $p < 0.05$. The data were statistically analysed in Statistica CZ 6.1 software.

Results and Discussion

FTIR Spectroscopy-Clay/Starch Interactions

FTIR analysis is a powerful tool to analyse, in a qualitative way, the interaction that occurs between a plasticizer, starch molecules and fillers. For the TPS and each of the blends, the spectra of both sides of the sample displayed the same number of peaks, and the positions and relative intensities of these peaks were identical. The FTIR spectra for TPS and certain blends are shown in Fig. **1**. The characteristic peaks for starch molecules and potential interactions with plasticizers through the bonding of hydrogen are described in Table **3**.

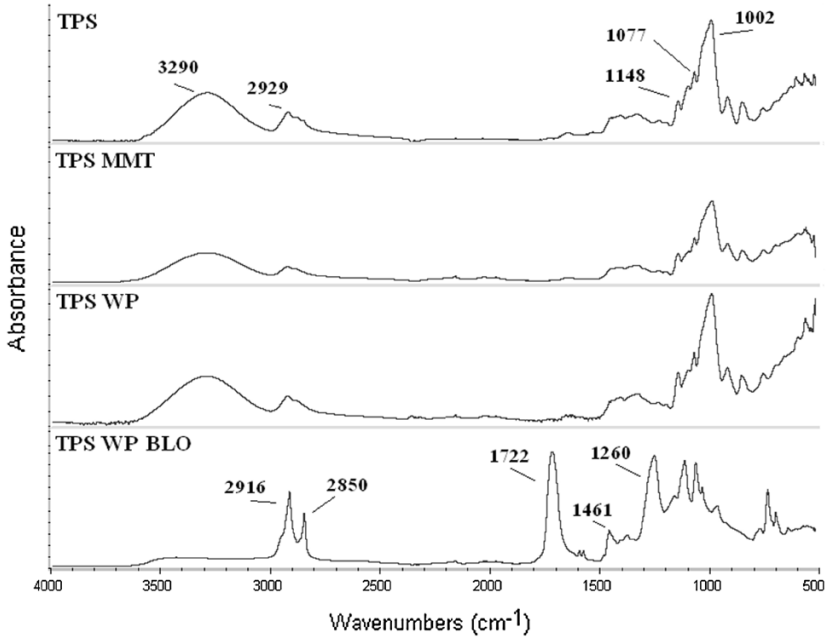

Fig. 1 Representative FTIR spectra for the TPS, blends and hydro-phobized blends. (TPS thermoplastic starch, TPS MMT thermoplastic starch/montmorillonite Cloisite Na^+, TPS WP thermoplastic starch/ waste paper, TPS WP BLO hydrophobized thermoplastic starch/waste paper)

Table 3 Wave numbers for C-O stretching, C-OH bonds and the stretching of C-H bonds in the TPS/clay blends

	Wavenumbers (cm^{-1})		
	C–O str	C–OH str	C–H str
TPS	1002.0	1103.5	2899.0
TPS MMT	995.2	1102.6	2894.5
TPS Lu-B	996.6	1101.9	2887.2
TPS S-B	999.1	1103.2	2889.5
TPS Ka	996.7	1102.5	2894.0
TPS Di	997.1	1102.5	2893.3
TPS SiPow	995.9	1101.2	2883.3

The broad peak at 3290 cm^{-1} is dominated by the stretching of the OH groups (inter- and intra-molecular). The peaks at 2929 and 2899 cm^{-1} relate to the C-H and CH_2 stretching of the anhydroglucose ring, which does not participate in thermoplasticization. The peaks at 1148 cm^{-1}, 1077 cm^{-1} and 1002 cm^{-1} were attributed by the authors to the C-O bond stretching of the C-O-H group in starch and the C-O bond stretching of the C-O-C group in the anhy-droglucose ring, respectively [**31**].

The spectra for the TPS/clay blends presented signals corresponding to TPS and clay particles, as anticipated (see, for example, Fig. **1**). However, slight changes in the modes below 800 cm^{-1} were observed. Similar results were reported by Castillo et al. [**11**], who studied the influence of adding clay to the structure of starch-based films. Interestingly, the intensities of the clay bands in the blends were relatively weak due to the low concentration of clay (5%). The same results were observed for the TPS WP specimen.

The band assignment for the FTIR spectrum of TPS WP, as hydrophobized by the boiled linseed oil (TPS WP BLO), is presented in Fig. **1**, where the TPS spectrum is compared with those of the samples. Several spectral changes typical for boiled linseed oil are visible: 2916 and 2850 cm^{-1} show the strong stretching of (C-H)CH_2; 1722 cm^{-1} reveals the strength of C=O; 1461 cm^{-1} presents strong bending of -CH_2; 1260 cm^{-1} refers to the medium stretching of C-C-O; 1164 cm^{-1} displays the strong stretching of C-O; 1100 cm^{-1} represents the medium stretching of O-CH_2-C; and 723 cm^{-1} demonstrates the strength of -(CH_2)n- with the wagging of (C-H)=CH [**32**].

In the presence of the clays as the filler, the stretching modes of the C-O and C-OH bonds of the starch, respectively, at 1002 cm^{-1} and 1103.5 cm^{-1} (Table **3**), shift towards lower wavelengths. These shifts are due to clay-starch interactions arising through the existence of hydrogen bonds, which are weaker than the chain-chain interactions in the starch. The stretching mode of the carbon skeleton of the starch chains at 2899 cm^{-1} is similarly affected (Table **3**), further confirming the weakening of the chain-chain interactions in the starch. These shifts in wavelength for blends containing the SiPow and Lu-B are greater than those caused by the presence of another clay, indicating an increase in silica-starch or Lu-B-starch interactions, probably due to the better dispersion of such clays [**33**].

Atomic Force Microscopy (AFM)

The degree and rate of biodegradation of polymeric materials not only depends on the type of polymer, stabilizer and plasticizer utilized, but also on the surface properties of the product. It has been shown that the roughness of the surface on a material influences the succession and composition of microorganisms colonizing said surface, as reflected in the rate of biological decomposition [**34**]. For this reason, we also decided to conduct AFM to study the surface topography and surface filler distribution (phase contrast) of the blends.

As shown in Fig. **2**, with respect to change in the roughness of the surface (parameter Sa), it was not possible to observe any major differences between the blends. This parameter ranged between 4-21 nm for all the mixtures, such minimal variance meaning the biodegradation of the TPS and blends had not been significantly influenced. This would suggest that the roughness of the surfaces of the TPS and blends and the extent of change undergone did not allow for a succession of microorganisms to settle on the surface; hence, no resultant increase occurred in the rate of biodegradation. In relation to the proportion of filler in the surface layer, phase-contrast imaging revealed that considerable dissimilarities were distinguishable between the blends (see Fig. **2**). The amount of filler at the phase boundary ranged between 1.4 and 54%. These changes in filler content at the phase boundary were determined by the surface energy of the dispersed particles with respect to the carrier matrix. Variations in this parameter did not correspond with other trends for water uptake, water solubility or biological degradation. Consequently, the authors did not discern that any dependence existed between distribution of the filler on the surface of the mixture and the biodegradability of the latter.

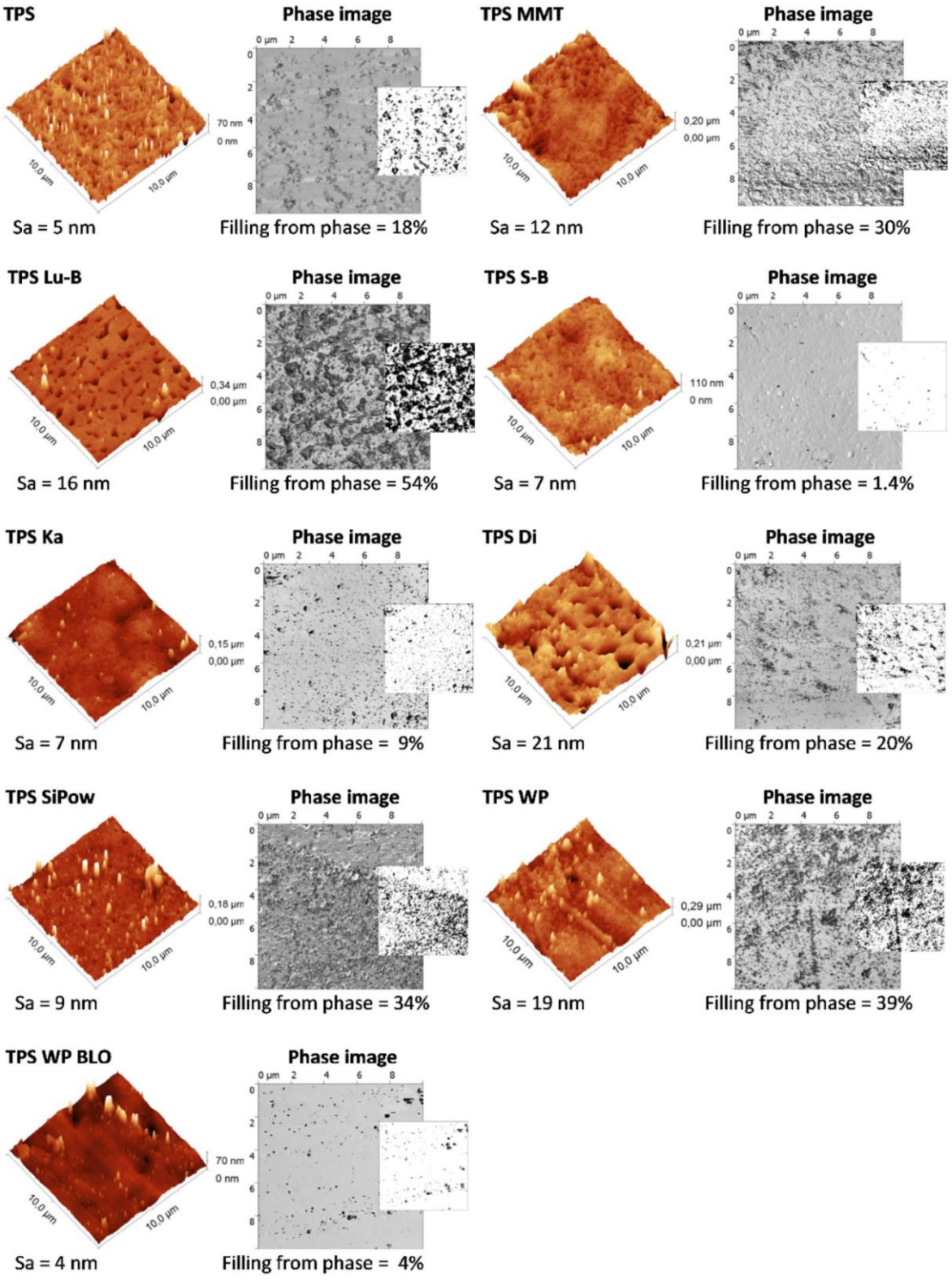

Fig. 2 Surface nano texture (colour images) and phase contrast (phase images) characterized by AFM. The small black-and-white pictures are previews of threshold phase images. (TPS thermoplastic starch, TPS MMT thermoplastic starch/montmorillonite Cloisite® Na^+, TPS S-B thermoplastic starch/Sabenil® bentonite, TPS Lu-B thermoplastic starch/Lutila® bentonite, TPS Ka thermoplastic starch/ kaolin, TPS Si_{Pow} thermoplastic starch/silica, TPS Di thermoplastic starch/diatomite, TPS WP thermoplastic starch/waste paper, TPS WP BLO hydrophobized thermoplastic starch/waste paper) (Color figure online)

Water Uptake Test

Although the water uptake of the TPS and blends plays an important role in biodegradation and any subsequent outcome in the environment, it is also significant for the long-term storage, handling and application of an eventual product made from the same material(s). A chief disadvantage of any starch is the strongly hydrophilic character it possesses. The hydroxyl groups present in its structure make it a polar substance that easily attracts water molecules from the environment. Interaction with water changes the biodegradation of materials based on thermoplastic starch, since it can weaken interactions between the starch molecules and bring about more flexible molecular motion, facilitating a retrogradation process [**4**].

Tests were conducted to determine the effects exerted by the source of the clay, adding WP or hydrophobization on the capacity for moisture sorption of the blends. In this context, the TPS and blends were placed in humidity chambers with 54% and 100% relative humidity (HR) at the room temperature of 25 ± 2 °C. The evolution of water absorption over time was followed for each sample as a function of time. Figure 3 shows the resulting sorption curves for the neat TPS and blends at both values of RH.

As a consequence of the glycerol content in the blends being the same, any differences observed were due to the presence and amount of clay or WP or the given state of dispersion or hydrophobization. The moisture absorption maximum was strongly dependent on the atmosphere of relative humidity and less reliant on the nature of the blends. Moreover, the moisture sorption maximum at 100% RH was raised by incorporating the clays, in agreement with results reported by other authors [**33**], ascribed to the fact that starch is more hydrophilic than clay. The greatest capacity for water uptake at 100% relative humidity was demonstrated by TPS Di (92.48%). In contrast, the lowest values were recorded for TPS SiPow (37.92%).

At 100% RH, the following experienced a drop in water uptake over time: TPS SiPow, TPS and all mixtures tested at 54% RH. Similar results were also obtained by Montero et al. [**4**], who described it as the retrogradation phenomena of the material. As mentioned above, the presence of water promotes the movement of the chains and encourages retrogradation. During this process, the materials tend to shed water and other volatiles, causing decrease in the weight of the material, resulting in the drop-off in the curve after reaching maximum. When samples are subjected to a relative humidity of 100%, respectively 54%, for more than 50 h, they suffer from swelling and become softer and opaque, and even turn yellow in shade [**4**].

In conclusion, all the blends were less hygroscopic at RH 54%, hence suitable for use in agriculture; for example, as packaging materials for controlled release of chemicals (pesticides, fertilizers).

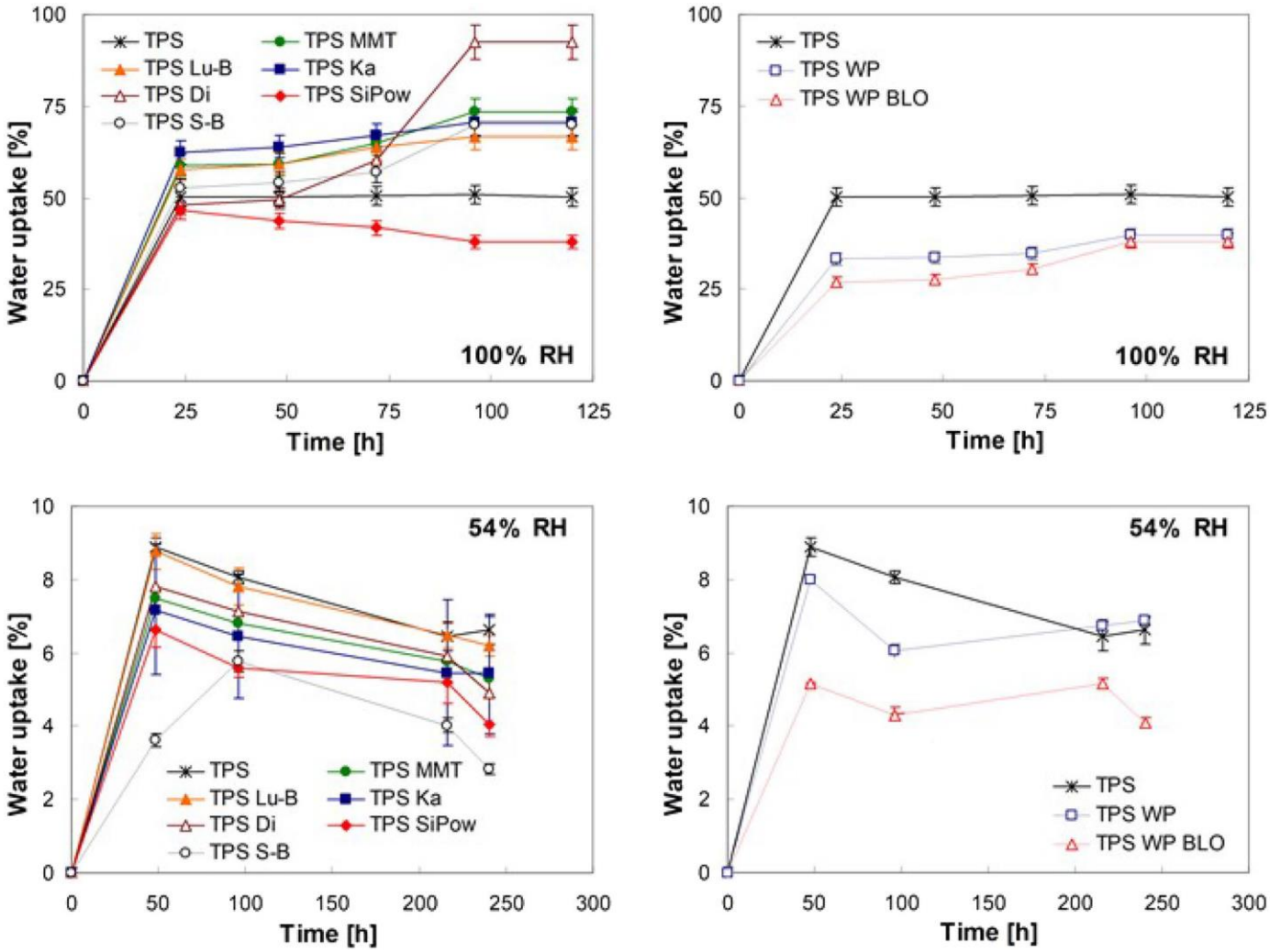

Fig. 3 Water uptake for the TPS and blends in per cent under conditions of relative humidity at 100% and 54% at laboratory temperature (average ± standard deviation; n = 5). (TPS thermoplastic starch, TPS MMT thermoplastic starch/montmorillonite Cloisite® Na^+, TPS S-B thermoplastic starch/Sabenil® bentonite, TPS Lu-B thermoplastic

Water Solubility

As for water uptake, the water solubility of the TPS and blends is crucial to the rate of biodegradation and the fate of the material in the given environment. Said water solubility in per cent at equilibrium, as determined at the laboratory temperature of 25 °C or 37 °C, is summarized in Table **4**.

The solubility in water of the TPS and blends took place in a single stage at 25 °C, and a level of equilibrium was reached after 10 days. The solubility of TPS at 25 °C was 30.2 ± 1.5%; adding a clay raised the extent of solubility by almost 15%. As anticipated, solubility was at its highest in TPS MMT, since Cloisite Na^+ montmorillonite is capable of a high degree of hydration. However, solubility values starch/Lutila® bentonite, TPS Ka thermoplastic starch/kaolin, TPS SiPow thermoplastic starch/silica, TPS Di thermoplastic starch/diato-mite, TPS WP thermoplastic starch/waste paper, TPS WP BLO hydro-phobized thermoplastic starch/waste paper) similar to those for TPS were recorded for the kaolin and kieselguhr blends (30.6 ± 1.5% and 29.9 ± 1.5%, respectively).

Table 4 Water solubility of the TPS and blends at different dissolution temperatures: 25 °C and 37 °C; in per cent at equilibrium (eq), (average ± standard deviation; n = 5)

Sample	25 °C (eq: 10 days)	37 °C (eq: 7 h)	
		1st stage	2nd stage
TPS	30.2 ± 1.5^{a}	34.8 ± 1.7^{a}	73.0 ± 3.7^{a}
TPS MMT	45.7 ± 2.3^{d}	37.1 ± 1.9^{a}	77.9 ± 3.9^{a}
TPS Lu-B	38.3 ± 1.9^{c}	45.1 ± 2.3^{c}	88.2 ± 4.4^{c}
TPS S-B	36.4 ± 1.8^{b}	46.4 ± 2.9^{c}	95.6 ± 4.8^{d}
TPS Ka	30.6 ± 1.5^{a}	38.0 ± 1.9^{a}	82.0 ± 4.1^{b}
TPS Di	29.9 ± 1.5^{a}	48.1 ± 2.4^{c}	84.9 ± 4.2^{b}
TPS SiPow	33.5 ± 1.7^{a}	37.3 ± 1.9^{a}	72.1 ± 3.6^{a}
TPS WP	38.7 ± 1.9^{c}	47.6 ± 2.4^{c}	82.1 ± 4.1^{b}
TPS WP BLO	27.2 ± 1.4^{b}	38.4 ± 1.9^{a}	96.2 ± 4.8^{d}

a' b'c' dValues with the same letter at the same column are not different statistically ($p < 0.05$)

In the case of kaolin, this was due to the distance between the layers being significantly less than for montmo-rillonite; note that no possibility exists for expansion (swelling) of the structure of kaolinite as it does for montmorillon-ite. As regards those containing diatomite, our findings can be attributed to the considerable sizes of the particles (dia-tomaceous shells) that remained intact and to the specific, relatively low, surface value for the same. No significant increase in solubility (38.7 ± 1.9%) was observed for TPS WP, despite it being characterized by high hydrophilicity. Hydrophobization of the surfaces of the mixtures resulted in their solubility being reduced by 10% in comparison with TPS WP. Hence, hydrophobization, as expected, contributed to increasing the resistance of the materials to water at 25 °C.

Solubility in water of TPS and the blends took place in two stages at 37 °C, and a level of equilibrium was reached after 7 h. The initial step of dissolution probably involved releasing the plasticizer, i.e. glycerol, from the mixtures, and only then (in the second step) did the starch actually dissolve. The water solubility of TPS at equilibrium equalled 73.0 ± 3.7%. Incorporating the majority of the fillers into TPS (5% w/w or 8% w/w) led to increase in water solubility at 37 °C in the blends. Solubility was at the highest in TPS S-B (95.6 ± 4.8%) and TPS WP BLO (96.2 ± 4.8%), whereas the lowest was seen in TPS SiPow (72.1 ± 3.6%).

The data obtained (Table **4**) and Tukey-Kramer test did not allow for elucidation as to why differences existed between the water solubility values for the samples. The only possible conclusion to be drawn is that the dissolution rate of all the mixtures is about 35 times higher at 37 °C than at 25 °C. We observed that hydrophobization did not exert a significant effect on the water solubility of the blends at 37 °C.

Biodegradation

Materials based on TPS are generally considered biodegradable, and for this reason many scientific papers have primarily focussed on studying the influence of components on the processing properties of the final product [**31**]. However, as can be deduced from past research, biodegradation does not only depend on the chemistry of the polymer, but also on the presence of the biological systems involved in the process. When investigating the biodegradability of polymeric materials, the effect of the environment cannot be neglected. Microbial activity, and thereby biodegradation, is influenced by the following: the presence of a microorganism, the availability of oxygen, the amount of available water, temperature and the chemical environment [**35**]. Hence, we decided to study the biological degradation of TPS materials modified by inorganic or organic micro/nano-fillers. Biodegradation was investigated with a view to where resultant products (household items) were likely to end up in wastewater settings, i.e. aerobic conditions (25 °C), respectively at the site of the anaerobic wastewater treatment machinery (37 °C), and in an agricultural chemistry context—soil at 25 °C with approximately 54% RH.

Biodegradation was evaluated via respirometric assays. The curves of the measured dependencies of D_{CO2} = f(t), D_{bod} = f(t) and DCH_4=f(t) were, unless otherwise indicated, typical of readily degradable starch-type substrates, and regressions were described by the equation for first-order kinetics of the substrates (the results obtained are summarized in Table **5**). It should be emphasized that the order of reaction is only empirical in magnitude, so is not significant in relation to the kinetics of the substrates. In essence, it describes the occurrence of relatively complicated processes with simple power functions, merely applicable within the limits of the given conditions.

Biodegradation in an Aqueous Aerobic Environment at 25 °C

As shown in Table 5, the mixtures containing clays demonstrated a decrease in the percentage of biodegradation by up to 10% compared to the decomposition of TPS. The highest degree of biodegradation was seen in TPS S-B (81.31 ± 0.23%) and TPS Ka (81.32 ± 0.24%). Meanwhile, TPS SiPow exhibited the longest decomposition time, with a half-life of 75.51 h and a lower percentage for decomposition (71.54 ± 0.88%). A lesser rate for total degradation was also observed for TPS MMT, TPS Di and TPS Lu-B. However, despite the above, adding a filler increased the rate and shortened the period for TPS biodegradation. Indeed, in this context, the most rapid mixture proved to be TPS MMT (- k = 13.85 ± 0.22 h^{-1}) with a half-life of 50 h.

TPS WP showed percentages for biodegradation similar to most of the clay-filled materials. However, its half-life was 70.59 h and the degradation rate only slightly exceeded than that of TPS (- k=9.82 ± 0.17 h^{-1} and - k=8.69 ± 0.12 h^{-1}), thus WP did not significantly contribute to increasing and accelerating the biodegradation of the blends.

The TPS WP BLO blend demonstrated the worst extent of biodegradability, in addition to which the biodegradation curve did not follow a course typically described by first-order kinetics. For TPS WP BLO, the percentage of biodegradation equalled approximately 28.8 ± 2.51% for 77 days. Of great import was the BLO, which was not subject to biodegradation under the given conditions, as evidenced by the control test (data not presented).

On the basis of the results given in Table **5**, it is appropriate to distinguish two different types of TPS material for the purposes of this study—materials with in-water dispersion clay fillers and those with non-dispersible fillers.

Table 5 Kinetic model parameters for the biodegradation of the TPS and blends (± SD) and half-life time

Sample	Dmax (%)	− k (10^{-3} h^{-1})	t_{lag} (h)		$t_{1/2}$ (h)
Aqueous aerobic conditions (activated sludge); duration of test: 75 days*[I]					
TPS	88.54 ± 0.32[a]	8.69 ± 0.12[a]	33.41 ± 0.62[a]		79.76[a]
TPS MMT	78.54 ± 0.22[c]	13.85 ± 0.22[d]	33.76 ± 0.69[a]		50.05[d]
TPS Lu-B	77.59 ± 0.58[c]	11.54 ± 0.39[c]	37.89 ± 1.46[b]		60.06[c]
TPS S-B	81.31 ± 0.23[b]	10.17 ± 0.15[b]	48.09 ± 0.79[d]		68.16[b]
TPS Ka	81.32 ± 0.24[b]	12.49 ± 0.20[c]	29.14 ± 0.78[b]		55.50[c]
TPS Di	79.94 ± 0.42[b]	9.78 ± 0.18[b]	27.79 ± 0.67[b]		70.87[b]
TPS SiPow	71.54 ± 0.88[c]	9.18 ± 0.37[a]	45.70 ± 1.52[c]		75.51[a]
TPS WP	79.41 ± 1.60[b]	9.82 ± 0.17[b]	50.02 ± 0.50[d]		70.59[b]
TPS WP BLO	28.80 ± 2.51[d]	Not equal to first-order kinetics for substrates			
Aqueous anaerobic conditions (digested sludge); duration of test: 55 days*[II]					
TPS	68.83 ± 3.44[a]	20.90 ± 0.68[a]	< 24 h	33.17[a]	
TPS MMT	68.80 ± 3.45[a]	21.90 ± 0.64[a]	< 24 h	31.65[a]	
TPS Lu-B	72.00 ± 3.25[a]	24.00 ± 0.32[b]	< 24 h	28.88[b]	
TPS S-B	76.56 ± 3.83[b]	23.14 ± 0.60[b]	< 24 h	29.95[b]	
TPS Ka	99.71 ± 4.99[d]	21.68 ± 0.65[a]	< 24 h	31.97[a]	
TPS Di	77.18 ± 3.86[b]	20.04 ± 0.72[a]	< 24 h	34.59[a]	
TPS SiPow	78.70 ± 3.94[b]	16.10 ± 1.05[c]	< 24 h	43.06[c]	
TPS WP	43.14 ± 2.16[c]	16.60 ± 0.99[c]	< 24 h	41.75[c]	
TPS WP BLO	46.83 ± 2.34[c]	15.23 ± 1.19[c]	< 24 h	45.49[c]	
Soil—aerobic conditions (2nd stage); duration of test: 25 days*[III]					
TPS	57.05 ± 0.28[a]	7.6 ± 0.15[a]	155.8 ± 1.4[a]	91.20[a]	
TPS MMT	56.17 ± 0.21[a]	8.2 ± 0.15[b]	148.3 ± 1.4[a]	84.53[b]	
TPS Lu-B	56.81 ± 0.23[a]	9.1 ± 0.18[c]	183.2 ± 1.4[c]	76.17[c]	
TPS S-B	82.52 ± 1.17[c]	4.0 ± 0.13[d]	40.6 ± 1.6[d]	173.29[d]	
TPS Ka	70.39 ± 0.37[b]	6.6 ± 0.12[b]	162.5 ± 1.1[b]	105.02[b]	
TPS Di	67.14 ± 0.33[b]	6.8 ± 0.12[b]	130.4 ± 1.2[c]	101.93[b]	
TPS SiPow	56.65 ± 2.83[a]	8.7 ± 0.09[c]	120.2 ± 1.2[c]	79.67[c]	
TPS WP	73.02[b]	Not equal to first-order kinetics for substrates			
TPS WP BLO	59.36[a]				

[a' b'c' d]Values with the same letter at the same column are not different statistically ($p < 0.05$)

**When a constant level of CO_2 (*[I]), BOD (*[III]) or CO_2 and CH_4 (*[II]) release was attained (plateau phase reached) and no further biodegradation was expected, the test was considered complete*

Dispersible fillers are characterized by a lamellar layered structure (MMT, Lu-B, S-B, Ka); incorporating the same into a polymeric matrix results in exfoliation and, concurrently, intercalation of starch and glycerol molecules into areas between the layers. For non-dispersible fillers, the only difference is that exfoliation of the filler structure may not occur or is even impossible since it does not consist of layers (Di, SiPow), unlike in clay minerals. As regards these materials, filler particles merely disperse within the polymeric matrix without any delamination effect. From this perspective, organic fillers of WP type are effectively equal to nondispersible fillers.

Consequently, it is possible to conclude that, on the basis of values for the rate constants of biodegradation (Table **5**), intercalation/exfoliation may exert some influence in biodegradation. The point is that, in terms of the velocity of aerobic biodegradation, utilizing in-water non-dispersible fillers appears to be a less appropriate solution, as they only support biological degradation to a very limited extent compared to the clay dispersible fillers applied. This theory finds support in studies by Bootklad and Kaewtatip [**13**] and Magalhaes and Andrade [**7**]. The former [**13**] observed that calcium carbonate (a non-dispersible filler) resulted in slower biodegradation of a TPS material. The latter [**7**] stated that adding MMT Cloisite 30B (a lamellar clay) led to a slight increase in the rate of biodegradation of a TPS material. However, further analyses would have to be performed (X-ray diffraction, differential scanning calorimetry) to arrive at any specific conclusions.

Biodegradation in an Aqueous Anaerobic Environment at 37 °C

Anaerobic digestion is a process involved within the disposal of waste food stuffs. These are often thrown away inside packaging materials made of a synthetic, non-biodegradable polymer, which it is usually necessary to remove manually prior to such digestion commencing. This issue could be avoided by utilizing packaging materials based upon TPS. Hence, it is advisable to carry out biodegradation tests under anaerobic conditions at 37 °C.

A number of polymeric materials possess the capacity to undergo relatively rapid degradation by aerobic microorganisms. Oxygen is crucial in such processes, since the degradation pathways depend on its presence. Nevertheless, the results of the experiments demonstrated that, for the TPS under study, it was temperature (37 °C) not the presence of oxygen which played a significant role in degradation. In this context, dissolution rates significantly changed for the TPS mixtures in the aqueous medium (Table **4**). This brought about significant increase in the rate of biodegradation and reduction in lag phase (< 24 h). The half-life of the material under anaerobic conditions was 50 per cent of that for biological decomposition in the aqueous aerobic medium, and one third of the duration for biological degradation in the soil environment.

Comparing the influence of the individual fillers on the anaerobic biodegradation of the mixtures reveals that positive results were only seen for mixtures containing clays. Comparison with TPS (- $k = 20.9 \pm 0.68\ h^{-1}$), regarding the time required for degradation, discloses that a negative effect was only observed in TPS SiPow (- $k = 16.10 \pm 1.05\ h^{-1}$). Both the rate and course of degradation of TPS MMT were almost identical to those observed for TPS, so it was concluded that the MMT filler did not exert any significant influence on the degradability of TPS. A positive outcome was reliably demonstrated in TPS Di, TPS S-B and TPS Ka. Indeed, all measurements showed higher values for the course and degree of degradation than those recorded for TPS. In particular, Ka (99.71%), Di (80.04%) and S-B (76.56%) would appear to be the most suitable fillers in terms of rate of degradation and degree of degradation.

TPS filled with WP, on the contrary, exhibited deterioration in all cases in relation to rate of degradability and TPS degradation. The least degree of degradation was recorded in TPS WP (43.14%). A slightly higher value was seen for TPS WP BLO (46.83%). The rate of biodegradation of TPS materials filled with WP was demonstrably lower than in the case of non-filled TPS, even though WP is considered a readily biodegradable material and frequently used to support biodegradation processes such as anaerobic digestion [**36**] and composting. A similar conclusion was reached by Mbarki et al. [**37**], who attributed the decreased rate and percentage of biodegradation to the higher extent of the crystalline phase in biocomposites containing cellulose-based fillers compared to clear biocomposites. Hydrophobization of the surface of the material by BLO, which biodegrades poorly under aerobic conditions, was discerned to be negligible under anaerobic conditions.

The data presented in Table **5** clearly show the trend of the influence exerted by the type of filler (in-water dispers-ible/non-dispersible) on the rate of biodegradation. In this context, utilizing non-dispersible fillers also appeared to be less appropriate in relation to the rate of anaerobic biodegradation, as these fillers did not contribute to promoting biodegradation as much as certain types of clay lamellar filler applied herein.

This could give rise to the presumption that good interca-lation/exfoliation of lamellar clays in a TPS matrix leads to increased diffusion of microorganisms with inherent water content into the material, as well as subsequent accelerated biodegradation. However, the values gauged for solubility and water absorption (Table **4** and Fig. **3**) do not support this theory. Indeed, further investigation would be necessary for clarification.

Biodegradation in Soil

Firstly, a soil burial test was chosen to assess the biodegradability of the TPS and blends in the soil environment, however, neither visual evaluation nor data obtained by gravimetric analysis yielded satisfactory results (high SD), hence the TPS and blends were subjected to respirometric tests (data are presented in Table **5**).

Said soil-burial test monitored the gradual decomposition of the TPS and blends in the soil environment for 7, 14, 18, 21 and 28 days of incubation. Figure **4** shows photographs taken of the TPS and blends, as a function of such periods of incubation. As mineralization progressed, the specimens showed gradual alteration in colour, thickness and roughness of surface in addition to increase in erosion. The TPS/ clay blends broke into pieces and easily crumbled when touched after 7 days. After 14 days, hardly any trace was found of almost every TPS/clay blend or the TPS WP sample that had not undergone hydrophobization, otherwise only a limited percentage of the same was discerned (images not presented). As for the blends of the hydrophobized BLO, biodegradation was noticeably slower.

We complimented visual evaluation of the biodegradation of the blends with SEM analysis. Figure **5** reveals that the surface morphology of the TPS and representative blends (TPS Di, TPS WP BLO) had changed after the 7-day soil respirometric test. The TPS demonstrated an irregular surface with holes, caused by the starch which had instigated biodegradation. In the case of TPS Di, agglomerates of the filler are visible (diatomaceous shells). Notably, the surface morphology of the hydrophobized blends also presented a rough surface with channels, although they showed a rough surface with channels, although they showed a more planar structure than the TPS.

This result indicated that hydrophobization hindered the penetration of water and microorganisms into the matrix. Moreover, the BLO increased the hydrophobicity of the matrix, which in turn diminished the degradation rate. These results corresponded with visual observations.

Fig. 4 Photographs of TPS and TPS/fillers before and after the biodegradation test (soil-burial test): TPS/clay blends - left; TPS/organic filler blends and hydrophobized TPS/organic filler blends - right. (TPS thermoplastic starch, TPS MMT thermoplastic starch/mont-morillonite Cloisite® Na^+, TPS S-B thermoplastic starch/Sabenil® bentonite, *TPS Lu-B* thermoplastic starch/Lutila® bentonite, *TPS Ka* thermoplastic starch/kaolin, *TPS SiPow* thermoplastic starch/silica, *TPS Di* thermoplastic starch/diatomite, *TPS WP* thermoplastic starch/ waste paper, *TPS WP BLO* hydrophobized thermoplastic starch/waste paper)

Regarding the blends that underwent the respirometric test, a 2-stage course (Fig. **6**) was witnessed, as anticipated by the authors. FTIR analysis proved that the first degree of breakdown corresponded to the release of glycerol. Figure **6** shows the representative FTIR spectra for TPS Lu-B over different time frames of degradation. The spectrum prior to the soil respirometric test shows a peak at 3290 cm^{-1}, which is related to hydroxyl groups present on the starch–glycerol films [**31**]. After 7 days of the soil respirometric test, the intensity of such a peak decreases. This is in agreement with the observation of leaching by glycerol during the first 7 days of biodegradation, and explains the first stage of degradation in the biodegradation curves from the respirometric test (Fig. **6**) [**38**]. The second stage comprised the course of the subsequent 14 days, characterized by a lower rate of weight loss, the degradation mechanism of which is linked with biological activity in the soil. Such biological degradation can also be observed in the FTIR spectra. In fact, the intensity of the peaks

associated with starch glycosidic linkages (1148–1077 cm^{-1}) decreased, indicating the action of α-amylase [**38**].

Comparing the influences of the individual fillers on the biodegradation of the blends in the soil environment (Table **5**) revealed that only those TPS blends containing Lu-B and Si-Pow showed significant higher degradation rates (- k = 9.1 ± 0.18 h^{-1} and - k = 8.7 ± 0.09 h^{-1}) than TPS (- k = 7.6 ± 0.15 h^{-1}), although the percentage of biodegradation exhibited comparable values (approx. 57%). The greatest percentage of biodegradation was seen in the TPS S-B mixture, 82.52 ± 1.17%; however, this was achieved at the cost of the lowest rate of decomposition of the material, with a half-life of almost twice that of TPS at 173 h. The blends showed a lag phase of biodegradation that ranged between 5 and 7 days, which could be anticipated for biodegradation in soil at 25 °C and RH 54%.

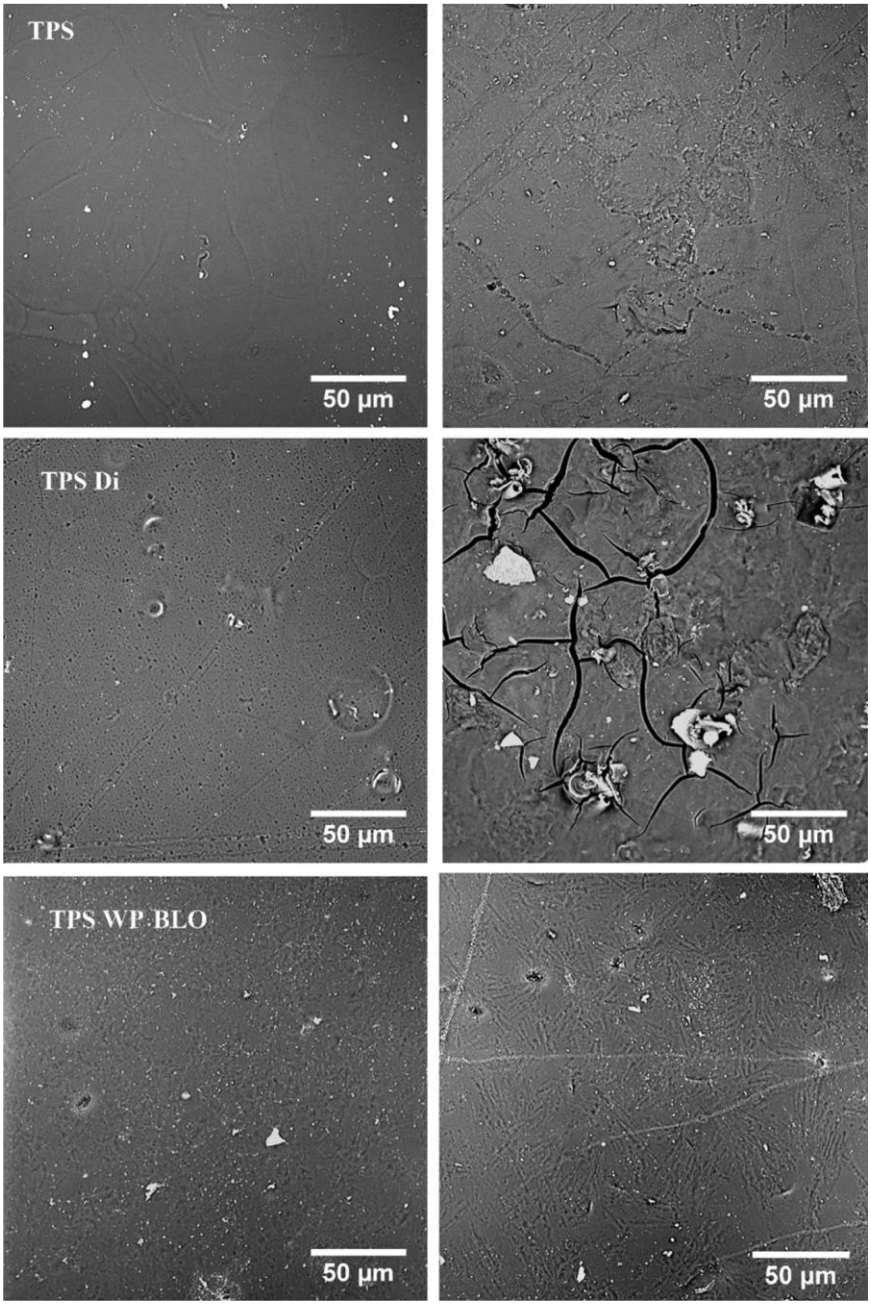

Fig. 5 Representative SEM for the TPS, TPS Di and TPS WP BLO blends before (left) and during (right) the soil-burial test—duration 7 days. (TPS thermoplastic starch, TPS Di thermoplastic starch/diatomite, TPS WP BLO hydrophobized thermoplastic starch/waste paper)

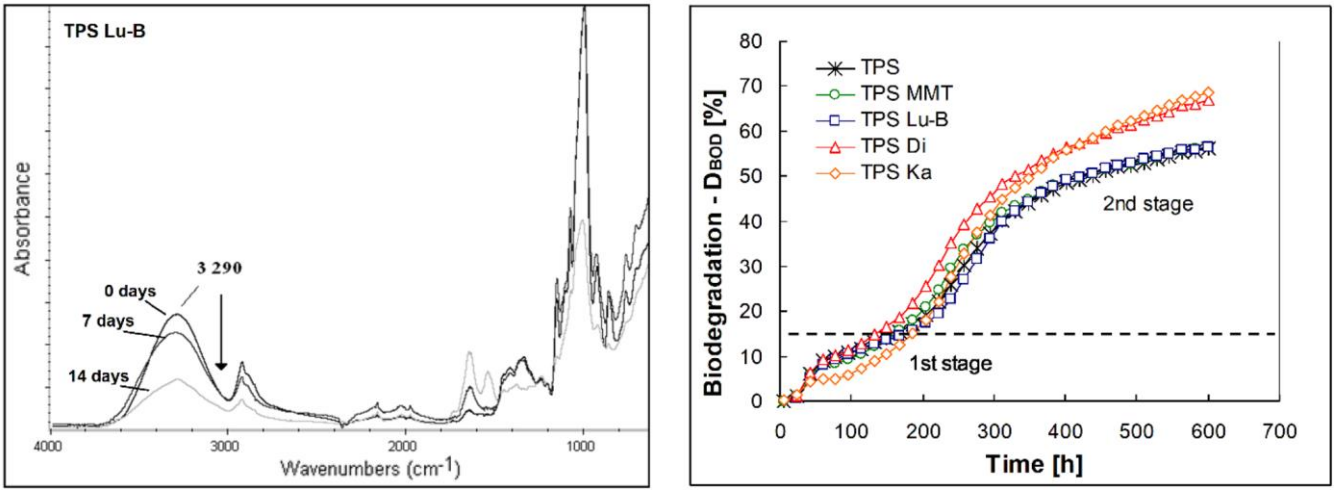

Fig. 6 Representative FTIR spectra for the TPS/clay blends (left) before the soil-burial test and after 7 days and 14 days in soil; biodegradation in soil—the graph for the respirometric test (right) shows representative biodegradation curves for selected TPS/clay blends and the TPS used as a control. (TPS thermoplastic starch, TPS MMT thermoplastic starch/montmorillonite Cloisite® Na^+, TPS Lu-B thermoplastic starch/Lutila® bentonite, TPS Ka thermoplastic starch/kaolin, TPS Di thermoplastic starch/diatomite)

In the case of the soil tests, no trend was demonstrated for effect exerted by the type of filler (dispersible/non-dispersible) on the biodegradation rates determined by the respirometric tests, despite Magalhaes and Andrade **[7]** and Bootklad and Kaewtatip [**13**] suggesting such a possibility existed. However, neither of said research teams carried out fully conclusive respirometric tests to evaluate biodegradation.

Biological decomposition of the blends filled with WP did not demonstrate patterns typical of first-order kinetics, and they were obviously slower than those for the blends supplemented with clay. The least percentage of degradation was seen (in agreement with the soil-burial test) for the hydrophobized blend containing WP.

Conclusion

Our study investigated two groups of mineral fillers, referred to either as in water-dispersible clays or in water non-dispersible inorganic fillers. The clay mineral fillers were characterized by a lamellar structure (MMT, Lu-B, S-B, Ka) and incorporating them into a polymeric matrix resulted in exfoliation and intercalation of the materials. As regards the non-dispersible fillers, the filler particles merely dispersed within the polymeric matrix. Waste paper was opted for as an organic filler; hence, in this context, it was also possible to include them in the group of non-dispersible fillers.

According to our results and the Tukey-Kramer test, it is possible to state that intercalation/exfoliation may have some importance within the biodegradation of a material based on TPS; in terms of the velocity of biodegradation, the use of non-dispersible fillers appears to be a less appropriate solution, since biological degradation is only supported to a very limited extent compared with the clay lamellar fillers applied herein. However, further analyses would need to be performed (X-ray diffraction, differential scanning calorimetry) to arrive at any specific conclusions.

The techniques opted for by the present team (AFM and FTIR) merely highlight the fact that surface topography, surface filler distribution and any interactions between the polymer matrix and clays are not factors crucial to the rate and degree of biodegradation of the TPS materials under study, even though FTIR analysis confirmed strong interactions between Lu-B/SiPow and starch. As regards the blends, there was virtually no connection between the intensity of clay-starch interactions, the roughness of the surface and the rate of fill of the phase boundary with the filler and the subsequent degradability of said blends.

In conclusion, filling a material with clays or organic substances of natural origin does not always mean that the favourable biodegradability of a resultant product is maintained. From the perspective of biodegradation, out of all the fillers under test, it would seem most appropriate (at the indicated concentrations) to modify the process and user properties of TPS with a type of a lamellar clay filler such as native, non-activated bentonite containing 75% mont-morillonite Lu-B. This kind of blend could be employed in applications with limited longevity, e.g. in agricultural chemistry and wastewater treatment equipment.

References

1. López OV, Castillo LA, Garcia MA, Villar MA, Barbosa SE (2015) Food packaging bags based on thermoplastic corn starch reinforced with talc nanoparticles. Food Hydrocolloids 43:18-24
2. Nafchi AM, Moradpour M, Saeidi M, Alias AK (2013) Thermoplastic starches: properties, challenges, and prospects. Starch-Starke 65(1-2):61-72
3. Lendvai L, Karger-Kocsis J, Kmetty Á, Drakopoulos SX (2016) Production and characterization of microfibrillated cellulose-reinforced thermoplastic starch composites. J Appl Polym Sci 133(2):42397
4. Montero B, Rico M, Rodríguez-Llamazares S, Barral L, Bouza R (2017) Effect of nanocellulose as a filler on biodegradable thermoplastic starch films from tuber, cereal and legume. Carbohydr Polym 157:1094-1104
5. Mondragón M, Mancilla JE, Rodríguez-González FJ (2008) Nanocomposites from plasticized high-amylopectin, normal and high-amylose maize starches. Polym Eng Sci 48(7):1261-1267
6. Chen B, Evans JR (2005) Thermoplastic starch-clay nanocomposites and their characteristics. Carbohydr Polym 61(4):455-463
7. Magalhaes NF, Andrade CT (2009) Thermoplastic corn starch/ clay hybrids: effect of clay type and content on physical properties. Carbohydr Polym 75(4):712-718
8. Magalhaes NF, Andrade CT (2010) Calcium bentonite as reinforcing nanofiller for thermoplastic starch. J Braz Chem Soc 21(2):202-208
9. Park HM, Li X, Jin CZ, Park CY, Cho WJ, Ha CS (2002) Preparation and properties of biodegradable thermoplastic starch/clay hybrids. Macromol Mater Eng 287(8):553-558
10. Lu P, Zhang M, Li C, Liu Z (2012) Effect of acid-modified clay on the microstructure and performance of starch films. Polym Plast Technol Eng 51(13):1340-1345
11. Castillo L, López O, López C, Zaritzky N, García MA, Barbosa S, Villar M (2013) Thermoplastic starch films reinforced with talc nanoparticles. Carbohydr Polym 95(2):664-674

12. Olivato JB, Marini J, Yamashita F, Pollet E, Grossmann MVE, Avérous L (2017) Sepiolite as a promising nanoclay for nanobiocomposites based on starch and biodegradable polyester. Mater Sci Eng C 70:296-302

13. Bootklad M, Kaewtatip K (2013) Biodegradation of thermoplastic starch/eggshell powder composites. Carbohydr Polym 97(2):315-320

14. Lopez O, Garcia MA, Villar MA, Gentili A, Rodriguez MS, Albertengo L (2014) Thermo-compression of biodegradable thermoplastic corn starch films containing chitin and chitosan. LWT Food Sci Technol 57(1):106-115

15. González K, Retegi A, González A, Eceiza A, Gabilondo N (2015) Starch and cellulose nanocrystals together into thermoplastic starch bionanocomposites. Carbohydr Polym 117:83-90

16. Martins IM, Magina SP, Oliveira L, Freire CS, Silvestre AJ, Neto CP, Gandini A (2009) New biocomposites based on thermoplastic starch and bacterial cellulose. Compos Sci Technol 69(13):2163-2168

17. Dogossy G, Czigany T (2011) Thermoplastic starch composites reinforced by agricultural by-products: properties, biodegradability, and application. J Reinf Plast Compos 30(21):1819-1825

18. Prachayawarakorn J, Ruttanabus P, Boonsom P (2011) Effect of cotton fiber contents and lengths on properties of thermoplastic starch composites prepared from rice and waxy rice starches. J Polym Environ 19(1):274-282

19. Duchek P, Dlouhý J, France P (2014) Composite biodegradable materials based on potato starch and micro/nanofillers. Eights Int Conf Mater Technol Model MMT 2014:1-44

20. Julinová M, Slavík R, Kalendová A, Smida P, Kratina J (2014) Biodeterioration of plasticized PVC/montmorillonite nanocomposites in aerobic soil environment. Iran Polym J 23(7):547-557

21. Ibrahim H, Farag M, Megahed H, Mehanny S (2014) Characteristics of starch-based biodegradable composites reinforced with date palm and flax fibers. Carbohydr Polym 101:11-19

22. Julinová M, Slavík R, Vyoralová M, Kalendová A, Alexy P (2018) Utilization of waste lignin and hydrolysate from chromium tanned waste in blends of hot-melt extruded PVA-starch. J Polym Environ 26(4):1459-1472

23. Bullock CM, Bicho PA, Zhang Y, Saddler JN (1996) A solid chemical oxygen demand (COD) method for determining biomass in waste waters. Water Res 30(5):1280-1284

24. ISO 15705:2002 Water quality—determination of the chemical oxygen demand—Small-scale dealer-tube method. Czech Standards Institute, Prague, Czech republic

25. Julinová M, Dvořáčková M, Kupec J, Hubáčková J, Kopčilová M, Hoffmann J, Alexy P, Nahálková A, Vašková I (2008) Influence of technological process on biodegradation of PVA/WAXY starch blends in an aerobic and anaerobic environment. J Polym Environ 16(4):241-249

26. ISO 17556:2012 Plastics-Determination of the Ultimate Aerobic Biodegradability of Plastic Materials in Soil by Measuring the Oxygen Demand in a Respirometer or the Amount of Carbon Dioxide Evolved. Czech Standards Institute, Prague, Czech republic

27. Rizzarelli P, Puglisi C, Montaudo G (2004) Soil burial and enzymatic degradation in solution of aliphatic co-polyesters. Polym Degrad Stabil 85(2):855-863

28. Pitter P, Chudoba J (1990) Biodegradability of organic substance in the aquatic environment, CRC Press, Boca Raton

29. Hoffmann J, Řezníčková I, Kozáková J, Růžička J, Alexy P, Bakoš D, Precnerová L (2003) Assessing biodegradability of plastics based on poly (vinyl alcohol) and protein wastes. Polym Degrad Stabil 79(3):511-519

30. Nunes MA, Castro-Aguirre E, Auras RA, Bardi MA, Carvalho LH (2019) Effect of babassu mesocarp incorporation on the biodegradation of a PBAT/TPS Blend. Macromol Symp 383(1):1800043

31. Zullo R, Iannace S (2009) The effects of different starch sources and plasticizers on film blowing of thermoplastic starch: correlation among process, elongational properties and macromolecular structure. Carbohydr Polym 77(2):376-383

32. Lazzari M, Chiantore O (1999) Drying and oxidative degradation of linseed oil. Polym Degrad Stabil 65(2):303-313

33. Mbey JA, Hoppe S, Thomas F (2012) Cassava starch-kaolinite composite film: Effect of clay content and clay modification on film properties. Carbohydr Polym 88(1):213-222

34. Wasserbauer R, Biological deterioration of buildings ABF-Arch 2002

35. Bastioli C (Ed) (2005) Handbook of biodegradable polymers. iSmithers Rapra Publishing, Akron.

36. Yen HW, Brune DE (2007) Anaerobic co-digestion of algal sludge and waste paper to produce methane. Biores Technol 98(1):130-134

37. Mbarki K, Fersi M, Louati I, Elleuch B, Sayari A (2019) Biodegradation study of PDLA/cellulose microfibres biocomposites by Pseudomonas aeruginosa. Environ Technol. https ://**doi. org/10.1080/09593330.2019.1643926**

38. Torres FG, Troncoso OP, Torres C, Diaz DA, Amaya E (2011) Biodegradability and mechanical properties of starch films from Andean crops. Int J Biol Macromol 48(4):603-606 Publisher's Note Springer Nature remains neutral with regard to jurisdictional claims in published maps and institutional affiliations.